KINEMATIC MODELLING AND ANALYSIS OF A WIRE-ACTUATED PARALLEL MANIPULATOR

Sureyya Sahin and Leila Notash

Department of Mechanical and Materials Engineering, Queen's University, Kingston, ON, Canada

notash@me.queensu.ca

Received June 2007, Accepted November 2007
No. 07-CSME-59, E.I.C. Accession 3028

ABSTRACT

The kinematic modelling and analysis of a 4 degrees of freedom wire-actuated parallel manipulator with redundant actuation is investigated. The manipulator employs combinations of rigid links, joints and wires. Hybrid actuation of joints and wires, two actuated joints and three actuated wires, is used. Position and first and second order kinematics of the closed-loop manipulator are formulated based on matrix exponentials. The transfer of first and second order kinematic variables, i.e., wire/joint velocities and accelerations, among the manipulator task space coordinates, active and passive joint coordinates and wire lengths are provided.

Keywords: Manipulator kinematics, wire-actuated manipulators, matrix exponentials

MODÈLE ET ANALYSE CINÉMATIQUES D'UN MANIPULATEUR ACTIVÉ PAR FIL

RÉSUMÉ

L'article examine un modèle et une analyse cinématiques d'un manipulateur parallèle activé par un fil de mobilité à quatre degrés avec une activation redondante. Le manipulateur emploie des combinaisons de liens, joints et fils rigides. L'activation hybride des joints et des fils, des deux joints activés et des trois joints activés, est utilisée. La position et la cinématique du premier et du deuxième ordre du manipulateur de boucle fermée sont formulées en fonction des exponentielles de matrice. Le transfert des variables cinématiques du premier et du deuxième ordre, à savoir les vélocités et les accélérations de fils et de joints, parmi les coordonnées d'espace de tâches du manipulateur, les coordonnées de joints actifs et passifs et les longueurs des fils, sont fournis.

Mots-clés : Cinématique du manipulateur, manipulateurs activités par fil, exponentielles de matrice

1. INTRODUCTION

Parallel manipulators are closed-loop mechanisms whose mobile platforms (end effectors) are connected to the base by means of at least two kinematic chains (legs/branches). Parallel manipulators have been investigated and utilized in many applications for half a century [1-3]. Wire-actuated parallel manipulators have been used for the advantages of being lightweight, low cost and having good load carrying capacity. For a mass suspended by wires in space, generally more than six wires are needed to equilibrate the mass against an external force/moment. Hence, the class of wire-actuated manipulators usually requires some means of redundant actuation to manipulate the mobile platform because of the inability of wires to exert forces in both directions along their lines of actions.

Kinematic analysis is required for mechanism design, in force and stiffness analysis, as well as in controller design and simulation of manipulators. The manipulator kinematics is used to relate the motion (displacement, velocity, acceleration) of joints to the end effector motion. Moving reference frames attached to individual links, e.g., Denavit-Hartenberg parameters [4], are used widely, and the relative motion of a frame with respect to another frame is formulated in the form of homogenous transformation matrices in a Cartesian coordinate system. Screw theory is commonly used for the first order kinematics and static analysis of manipulators to establish the kinestatic relations [5, 6]. The main advantage of the screw theory is the physical interpretation of the motion (twist) of the manipulator and the forces and moments (wrench) applied/resisted by the manipulator. Matrix exponentials, which are obtained from Lie groups and algebra associated with the motion in a coordinate system, are also being used in kinematic analysis of robot manipulators, e.g., in [7]. Matrix exponentials provide compact representation of the rigid body motion, e.g., [8-10], so that the physical interpretation of the motion of manipulators can be performed.

The kinematic analysis of parallel manipulators is widely studied in literature due to the complexity that arises because of employing passive joints, which usually are not measured, in addition to active joints. In general, the solution of inverse finite kinematics (displacement analysis) of parallel manipulators is more straightforward compared to forward kinematics. Kinematic analysis of closed-loop manipulators could be based on loop closure equations from which a relation between the joint variables of the manipulators is obtained. Additionally, the position and orientation (pose) of the mobile platform of a parallel manipulator in terms of individual branches can be used to obtain a relation between the joint variables and mobile platform coordinates.

The application of rigid body kinematics to a wire-actuated parallel robot manipulator is studied in this article. The manipulator employs a rigid branch to constrain the motion of mobile platform in yaw and roll rotations. The degrees of freedom (DOF) and constraints of the closed-loop manipulator are discussed. Lie groups and algebras, matrix exponentials applied to rotation groups, and mappings of the first and the second order kinematic variables among the task space coordinates, active and passive joint coordinates and wire lengths are investigated. The kinematic analysis reported in this article has been used in force and stiffness analyses of the manipulator [11, 12].

2. RIGID BODY MOTION APPLIED TO A WIRE-ACTUATED PARALLEL MANIPULATOR

Applications of theory of kinematics are illustrated in this section for a 4 DOF (three translations and pitch rotation) wire-actuated parallel manipulator (Figure 1). The manipulator was designed in [13] for soil sampling applications at planetary explorations based on the specifications provided by MD Robotics, Ltd., developer of Space Station Remote Manipulator System (also known as Canadarm2). This mechanism consists of a rigid branch, which has a 4 DOF, and is controlled by two actuated joints and three wires. The forward and inverse position (displacement), velocity and acceleration analyses are performed for the rigid branch and the wires. The transfer of coordinates is formulated to write the passive joint rates, active joint/wire rates and mobile platform coordinates in terms of each other.

The rigid branch connects the centre of the mobile platform to the base, and consists of a parallelogram mechanism, which is connected to the base, and a link for connecting the mobile platform to the parallelogram mechanism. The rigid branch consists of seven joints, where the two joints closest to the base, at the origins of coordinate frames O_0 and O_1, are actuated. Additionally, three wires attached to points A_i on the base, and points B_i on the moving links, are used to control the mobile platform. The wires are driven by the motor and drum assembly at points A_i as can be seen from Figure 1.

The parallelogram mechanism of the rigid branch, shown in Figure 2(a), has two degrees of freedom. This linkage is kinematically similar to the spatial four-bar mechanisms with layout of two spherical joints at the base and two revolute joints on the coupler, with an idle degree of freedom, which occurs due to the coincident rotation axis of the spherical joints. This parallelogram mechanism is over-constrained due to the usage of only revolute joints as

for $n = 5$ links, $j = 5$ joints and $f_i = 1$ for revolute joint i, the number of equations $E = 6(n-1) = 24$ is less than the number of constraints $V = \sum_{i=1}^{j=5} (6 - f_i) = 25$.

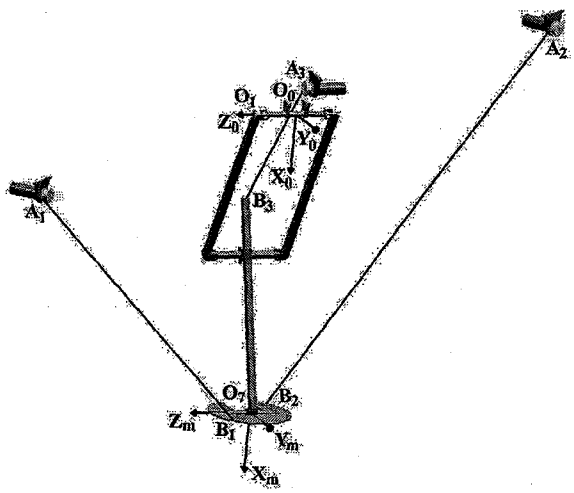

Figure 1 Considered 4 degrees of freedom wire-actuated parallel manipulator.

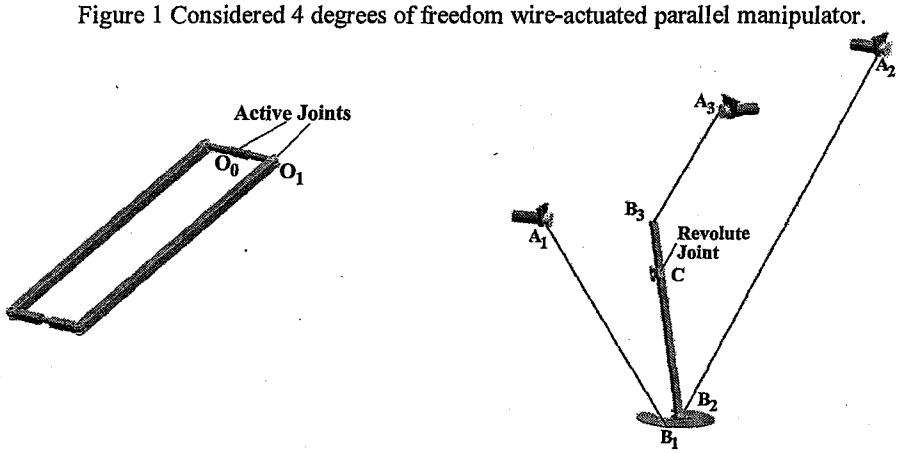

(a) (b)

Figure 2 (a) Parallelogram mechanism, (b) Serial mechanism of the wire-actuated parallel manipulator.

The serial mechanism (Figure 2(b)) consists of two serially connected links, one of which is connected to the coupler of the parallelogram mechanism with the revolute joint at C and the other link is the mobile platform. Three wires are attached to this linkage to actuate the mechanism; two wires are attached to points B_1 and B_2 on the mobile platform to control the revolute joint at O_7 (Figure 1), and the third wire is attached to point B_3. Thus, an additional wire is used to maintain the internal forces. As opposed to conventional force-closure mechanisms in which a rigid object is grasped by contact forces, the serial mechanism consists of two rigid links interconnected by a revolute joint.

The kinematic analysis of the mechanism is investigated by considering the motion of the wires and the rigid branch separately. Kinematics of the rigid branch is formulated based on the Denavit-Hartenberg coordinate frames. The wires in tension are treated such that at their attachment points to the base they have two rotational degrees of freedom and can make a translational motion along the wire axes determined by the line joining the corresponding

attachment points; the wires can make a spherical motion centered at the attachment point to the rigid branch. That is, the wires in tension are modelled such that they are equivalent to a universal-prismatic-spherical linkage.

2.1. Mobility Analysis

The degrees of freedom of the rigid branch can be calculated using the generalized mobility equation (Grübler's equation). However, due to the special geometry of some mechanisms, including the rigid branch, this equation does not provide correct mobility [14-16]. The degrees of freedom of the rigid branch as calculated using Grübler's equation, $F = 6(n-1) - \sum_{i=1}^{j}(6-f_i)$, gives $F = 1$ for $n = 7$ links, $j = 7$ joints and all the joints having one degree of freedom ($f_i = 1$). The formula $F = F_i + F_r = F_0 + M + F_c - F_p$ of [14] can be used to calculate the correct degrees of freedom of the mechanism. Considering this equation, $F_0 = 1$ is calculated from Grübler's equation. Also, the total idle degrees of freedom F_r is zero since the revolute joint axes are not collinear. There is one closed-loop due to the parallelogram mechanism, so the total over closing constraints which are used to give additional support to the mechanism without changing its degrees of freedom is 1 ($F_c = 1$). The general constraints M are 2 since the mobile platform of the rigid branch cannot rotate about two of the axes of the fixed coordinate system. The total passive degrees of freedom are zero ($F_p = 0$) as there are no vanishing joint variables during the velocity analysis. Thus, the degrees of freedom of the mechanism can be calculated as $F = 4$. The apparent mobility is $F_i = F - F_r = 4$. This result is the same as what the group theory (e.g., [17]) would predict for this branch. That is, a layout consisting of a parallelogram mechanism with revolute joints on the base and on the coupler links, both joints lying on the plane of the parallelogram, followed by another revolute joint being parallel to these two revolute joints (which is a Schönflies-motion generator) would have 4 DOF (three translations and one rotation).

2.2. Position Analysis

As has been discussed in [9], the rigid body transformation can be defined as a mapping $\phi : \Re^3 \rightarrow \Re^3$ such that the distance between any two points on the body and the orientation of points relative to each other are preserved. Rigid body motions are isometries that preserve the distance in space, and can be described by means of group theory. The orthogonal group, denoted by $O(n)$, is the group of $n \times n$ matrices such that $\boldsymbol{R}^T\boldsymbol{R} = \boldsymbol{R}\boldsymbol{R}^T = \boldsymbol{I}$. The group of rotations in Euclidean space is called the special orthogonal group $SO(3)$. Every rotation can be fully described by an axis and a rotation angle $(\boldsymbol{n}, \theta)$, i.e., by three parameters. $SO(3)$ is a compact group since the parameters that it describes are closed and bounded, however, it is not an abelian group since it is not possible to obtain the same orientation by commuting the sequence of rotations. This group can be described by:

$$SO(3) = \left\{\boldsymbol{R} \in \Re^{3\times 3} \mid \boldsymbol{R}\boldsymbol{R}^T = \boldsymbol{R}^T\boldsymbol{R} = \boldsymbol{I}, |\boldsymbol{R}| = 1\right\} \tag{1}$$

The $SO(3)$ group is an isometry, therefore $\|\boldsymbol{R}(\boldsymbol{a}-\boldsymbol{b})\| = \|\boldsymbol{a}-\boldsymbol{b}\|, \boldsymbol{a},\boldsymbol{b} \in \Re^3$ and $\boldsymbol{R}(\boldsymbol{a}\times\boldsymbol{b}) = \boldsymbol{R}\boldsymbol{a}\times\boldsymbol{R}\boldsymbol{b}, \boldsymbol{a},\boldsymbol{b} \in \Re^3$.

Establishing the groups for rotation and translation, the rigid body motion can be investigated in the Euclidean space. If the position and orientation of a rigid body attached frame with respect to a fixed coordinate system are respectively denoted as $\boldsymbol{r}$ and $\boldsymbol{R}$, using the special Euclidean group, the configuration space of body is expressed as:

$$SE(3) = \left\{(\boldsymbol{r}, \boldsymbol{R}) \mid \boldsymbol{r} \in \Re^3, \boldsymbol{R} \in SO(3)\right\} \tag{2}$$

Thus, $(\boldsymbol{r}, \boldsymbol{R}) \in SE(3)$ completely specifies the configuration of the rigid body. Then the position of a point on the rigid body is defined in the fixed frame using the affine mapping as ${}^0\boldsymbol{p} = \boldsymbol{r} + \boldsymbol{R}\boldsymbol{d}$. Using the homogenous point coordinates, the homogenous representation of this mapping is:

$$\begin{bmatrix} {}^0\boldsymbol{p} \\ 1 \end{bmatrix} = \begin{bmatrix} \boldsymbol{R} & \boldsymbol{r} \\ \boldsymbol{0} & 1 \end{bmatrix} \begin{bmatrix} d_1 \\ d_2 \\ d_3 \\ 1 \end{bmatrix} = \boldsymbol{A} \begin{bmatrix} \boldsymbol{d} \\ 1 \end{bmatrix} \tag{3}$$

The Lie algebra associated with the special orthogonal group and special Euclidean group are defined respectively as $so(3)$ and $se(3)$:

$$so(3) = \left\{\boldsymbol{w} \in \mathcal{R}^3 \mid \tilde{\boldsymbol{w}}^T = -\tilde{\boldsymbol{w}}\right\} \tag{4}$$

$$se(3)=\left\{\begin{bmatrix}\tilde{w} & v\\ 0 & 0\end{bmatrix} \mid \tilde{w}\in so(3), v\in \Re^3\right\} \tag{5}$$

where $\tilde{w}$ is the skew symmetric tensor for the angular velocity of the rigid body. The matrix exponentials obtained from kinematic analysis are generally one of the bases in $so(3)$ or $se(3)$. The basis given for $so(3)$ induces the rotation matrices in $SO(3)$ as:

$$R_x(\theta)=e^{\tilde{i}\theta},\ R_y(\theta)=e^{\tilde{j}\theta},\ R_z(\theta)=e^{\tilde{k}\theta} \tag{6}$$

Some of the important properties of the exponential mapping and skew symmetric matrices in $SO(3)$ and $so(3)$ are given in [7, 9]. The Lie algebra $se(3)$ induces a rigid body motion in $SE(3)$. The exponential mapping describes the motion of the rigid body in $SE(3)$ from an initial position and orientation with respect to the fixed reference frame. The Lie algebra $se(3)$ is isomorphic to twist motion, and the twist the rigid body receives can be related to Lie algebra $se(3)$ associated with its Lie group. Thus, for any twist $\xi\in se(3)$ in ray coordinates:

$$\hat{\xi}=\begin{bmatrix}\tilde{w} & v\\ 0 & 0\end{bmatrix}\rightarrow \xi=\begin{bmatrix}w\\ v\end{bmatrix}=\Delta\begin{bmatrix}v\\ w\end{bmatrix} \tag{7}$$

where Δ is the shift operator. The linear motion generated by the twist of a point on the rigid body can be written as $v=-w\times r+p_a w$, where p_a is the pitch of screw. Then the following expression can be obtained:

$$e^{\hat{\xi}\theta}=\begin{bmatrix}e^{\tilde{w}\theta} & (I-e^{\tilde{w}\theta})r+p_a\theta w\\ 0 & 1\end{bmatrix} \tag{8}$$

The exponential map created by this twist is a one parameter subgroup representing the infinitesimal twist motion which consists of a rotation about the axis of the screw and a translation parallel to the screw axis. Consequently, any rigid body motion can be written in terms of the exponential matrix using a twist about a screw. The exponential matrix in $SE(3)$ is surjective (onto mapping) on the set of twists as more than one instantaneous twist can produce the same rigid body motion.

Rigid Branch

The zero configuration of the rigid branch indicating reference frames 0, 1, 2, 3, 6 and 7 attached to links 0, 1, 2, 3, 5 and the mobile platform respectively are shown in Figure 3(a). The Denavit-Hartenberg parameters [18] of the mechanism are listed in Table 1, where θ_i, d_i, a_i and α_i represent the joint angle, joint offset, effective link length and twist angle, respectively. A fixed reference frame is attached at point O_0 to the base. Additional reference frames are employed to formulate the motion of link 4 relative to link 1 (frame 5), and link 3 relative to link 4 (frame 4). The relative joint angles between these reference frames are denoted by θ_4 and θ_5, respectively.

The orientation of the mobile platform can be written in terms of the parameters in Table 1 as $R_{0,m}=R_{0,7}=e^{\tilde{k}\theta_1}e^{\tilde{i}\frac{\pi}{2}}e^{\tilde{k}\theta_2}e^{\tilde{k}\theta_3}e^{-\tilde{i}\frac{\pi}{2}}e^{\tilde{k}\theta_6}e^{\tilde{k}\theta_7}$, which can be simplified using properties of the matrix exponentials, i.e., $e^{\tilde{i}\frac{\pi}{2}}e^{\tilde{k}\theta_2}e^{\tilde{k}\theta_3}e^{-\tilde{i}\frac{\pi}{2}}=e^{\tilde{i}\frac{\pi}{2}}e^{\tilde{k}\theta_{23}}e^{-\tilde{i}\frac{\pi}{2}}=e^{-\tilde{j}\theta_{23}}$ where $\theta_{23}=\theta_2+\theta_3$, as:

$$R_{0,m}=e^{\tilde{k}\theta_1}e^{-\tilde{j}\theta_{23}}e^{\tilde{k}\theta_{67}} \tag{9}$$

The position of the origin of the coordinate system attached to mobile platform at O_7 can be written as $p=d_1k_0+a_2i_2-d_6k_3+a_6i_6$, where d_1, a_2, d_6 and a_6 are the Denavit-Hartenberg parameters listed in Table 1, and i, j, k are unit vectors. When expressed in the fixed frame, p becomes:

$${}^0p=d_1k_0+a_2R_{0,2}i-d_6R_{0,3}k+a_6R_{0,6}i \tag{10}$$

where the rotation matrices are defined as $R_{0,2}=e^{\tilde{k}\theta_1}e^{\tilde{i}\frac{\pi}{2}}e^{\tilde{k}\theta_2}$, $R_{0,3}=R_{0,2}e^{\tilde{k}\theta_3}e^{-\tilde{i}\frac{\pi}{2}}=e^{\tilde{k}\theta_1}e^{-\tilde{j}\theta_{23}}$, $R_{0,6}=R_{0,3}e^{\tilde{k}\theta_6}=e^{\tilde{k}\theta_1}e^{-\tilde{j}\theta_{23}}e^{\tilde{k}\theta_6}$.

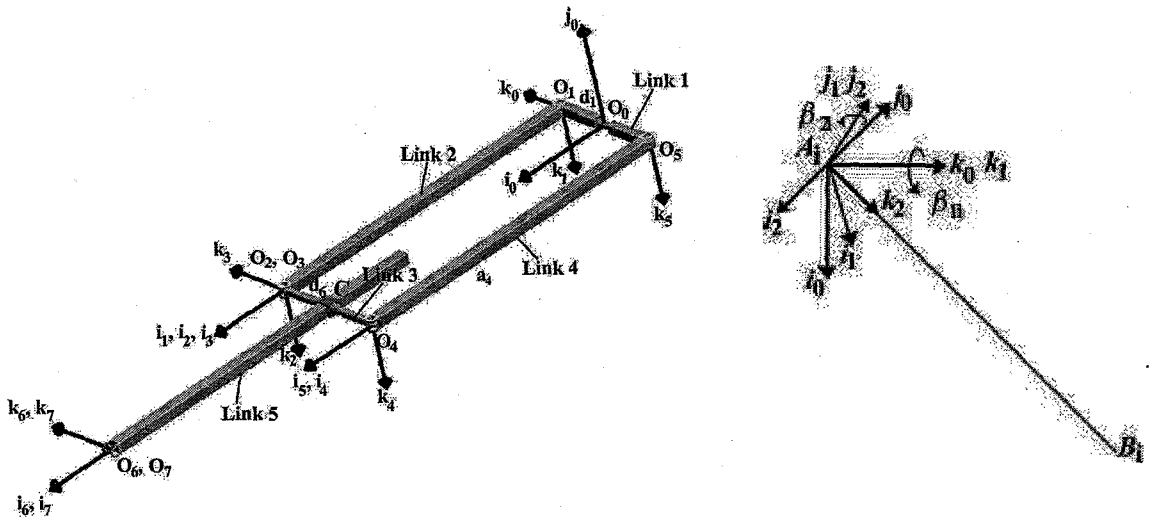

Figure 3 (a) Zero configuration of the rigid branch, (b) Rotating frames attached to a wire at the base.

Table 1 Denavit-Hartenberg parameters of the rigid branch.

Link	θ_i	d_i	a_i	α_i
1	θ_1	$d_1 = 0.1$ m	0	$\alpha_1 = \pi/2$
2	θ_2	0	$a_2 = 0.61$ m	0
3	θ_3	0	0	$\alpha_3 = -\pi/2$
5	θ_6	$d_6 = -0.1$ m	$a_6 = 0.48$ m	0
6	θ_7	0	0	0

Expanding equation (10), the position equation can be obtained in terms of the joint variables as:

$$ {}^0\boldsymbol{p} = \begin{bmatrix} a_2\cos(\theta_2)\cos(\theta_1) + a_6\cos(\theta_{16}) \\ a_2\cos(\theta_2)\sin(\theta_1) + a_6\sin(\theta_{16}) \\ a_2\sin(\theta_2) + d_1 - d_6 \end{bmatrix} \tag{11} $$

where $\theta_{16} = \theta_1 + \theta_6$. The closed loop provided by the parallelogram mechanism can be utilized to relate the passive joint variables to the active joint variables. The loop closure equation for the parallelogram mechanism at point O_4, $d_1\boldsymbol{k}_0 + a_2\boldsymbol{i}_2 - 2d_6\boldsymbol{k}_3 = -d_1\boldsymbol{k}_0 + a_4\boldsymbol{i}_4$, can be resolved into the fixed frame as:

$$ 2d_1\boldsymbol{k}_0 + a_2\boldsymbol{R}_{0,2}\boldsymbol{i} - 2d_6\boldsymbol{R}_{0,3}\boldsymbol{k} - a_4\boldsymbol{R}_{0,4}\boldsymbol{i} = \boldsymbol{0} \tag{12} $$

where $a_4 = a_2$ is the effective link length along the i-axis of coordinate frame 4. Equation (12) consists of three scalar equations, the first and third equations are as follows:

$$ a_2\cos(\theta_2) + 2d_6\sin(\theta_{23}) - a_4\cos(\theta_5) = 0 \tag{13} $$

$$ 2d_1 + a_2\sin(\theta_2) - 2d_6\cos(\theta_{23}) - a_4\sin(\theta_5) = 0 \tag{14} $$

Equations (13) and (14) can be used to solve for θ_3 and θ_5 as $\theta_5 = \theta_2$ and $\theta_3 = -\theta_2$ (also $\theta_4 = -\theta_2$). Then equation (9) reduces to:

$$ \boldsymbol{R}_{0,7} = e^{\tilde{k}\gamma} = \begin{bmatrix} \cos(\gamma) & -\sin(\gamma) & 0 \\ \sin(\gamma) & \cos(\gamma) & 0 \\ 0 & 0 & 1 \end{bmatrix} \tag{15} $$

where $\gamma = \theta_{167} = \theta_1 + \theta_6 + \theta_7$ is the pitch angle of the mobile platform. Given the pose of the mobile platform, the joint variables can be found. Equation (10) can be simplified as:

$$^0\boldsymbol{p} = e^{\tilde{\boldsymbol{k}}\theta_1}\left(a_2 e^{\tilde{\boldsymbol{i}}\frac{\pi}{2}} e^{\tilde{\boldsymbol{k}}\theta_2}\boldsymbol{i} + a_6 e^{\tilde{\boldsymbol{k}}\theta_6}\boldsymbol{i}\right) + (d_1 - d_6)\boldsymbol{k} \tag{16}$$

For $\boldsymbol{p}^* = {}^0\boldsymbol{p} - (d_1 - d_6)\boldsymbol{k}$ and defining $b_1 = p_z^*/a_2$, the joint variable θ_2 can be calculated as:

$$\theta_2 = atan2\left(b_1; \sigma\sqrt{1-b_1^2}\right), \sigma = \pm 1 \tag{17}$$

Because of the joint limits, $-\pi/2 \le \theta_2 \le \pi/2$ is considered. Joint variable θ_6 can be found as:

$$\theta_6 = \sigma cos^{-1}\left(\frac{p_x^{*2} + p_y^{*2} - a_6^2 - (a_2 cos(\theta_2))^2}{2a_2 a_6 cos(\theta_2)}\right) \tag{18}$$

Both solutions for θ_6 are considered since there is no joint limit. Joint variable θ_1 can be calculated as:

$$\theta_1 = 2atan2\left(\left(-p_x^* + \sigma\sqrt{p_x^{*2} + p_y^{*2} - (a_6 sin(\theta_6))^2}\right); \left(p_y^{*2} + a_6 sin(\theta_6)\right)\right) \tag{19}$$

The expression for θ_7 can be found from the orientation equation (15) as:

$$\theta_7 = \gamma - \theta_1 - \theta_6 \tag{20}$$

Wire Mechanism

Given the pose of the mobile platform, the kinematic parameters of the wires can be found in a similar manner. The wire lengths can be calculated by using the closed loops established by the wires. From Figures 1 and 2, the loop closure equations can be written as:

$$\boldsymbol{O_0A_i} + \boldsymbol{A_iB_i} = \boldsymbol{O_0O_7} + \boldsymbol{O_7B_i}, \; i = 1,2 \tag{21}$$

$$\boldsymbol{O_0A_3} + \boldsymbol{A_3B_3} = \boldsymbol{O_0C} + \boldsymbol{CB_3} \tag{22}$$

The wire vectors $\boldsymbol{l_i} = \boldsymbol{A_iB_i}$ for $i = 1,2$, can be found relative to the fixed frame as:

$$\boldsymbol{l_i} = {}^0\boldsymbol{p} + \boldsymbol{R}_{0,7}\boldsymbol{O_7B_i} - \boldsymbol{O_0A_i}, \; i = 1,2 \tag{23}$$

Equation (22) can be expanded and rearranged to find the length of wire 3 in terms of the joint variables of the rigid branch as:

$$\boldsymbol{l_3} = \left(a_2 cos(\theta_2)cos(\theta_1) - a_{6p}cos(\theta_{16})\right)\boldsymbol{i}_0 + \left(a_2 sin(\theta_2)sin(\theta_1) - a_{6p}sin(\theta_{16})\right)\boldsymbol{j}_0 + (d_1 - d_6)\boldsymbol{k}_0 - \boldsymbol{O_0A_3} \tag{24}$$

where $a_{6p} = \|\boldsymbol{CB_3}\|$. From equations (23) and (24), the wire lengths and unit vectors $\boldsymbol{n_i}$ associated with the line of action of each wire can be calculated.

Additionally, three coordinate frames with coincident origins at the base A_i (Figure 3(b)) are used for calculating the unit vector along each wire. From fixed frame $\{O_0\}$, the third frame which moves with the wire is obtained by two rotations. The coordinate system $\{O_0\}$ is located such that its origin is at A_i while its axes are parallel to the fixed frame located on the rigid branch at O_0. Then $\{O_1\}$ is obtained by a rotation about $\boldsymbol{k}_0$ by an angle β_{1i}. $\{O_2\}$ is obtained by a rotation about $\boldsymbol{j}_1$ by an angle β_{2i}. Thus a motion identical to that of a universal joint is obtained.

Thus, the wire vector $\boldsymbol{n_i}$ can be written with respect to the fixed frame as $\boldsymbol{n_i} = \boldsymbol{R}_{0,2i}\boldsymbol{k} = e^{\tilde{\boldsymbol{k}}\beta_{1i}} e^{\tilde{\boldsymbol{j}}\beta_{2i}}\boldsymbol{k}$. The wire vector $\boldsymbol{n_i}$ can be calculated relative to $\{O_0\}$ from the known attachment points on the mobile platform and on the base and in terms of the kinematic variables as:

$$\boldsymbol{n_i} = cos(\beta_{1i})sin(\beta_{2i})\boldsymbol{i}_0 + sin(\beta_{1i})sin(\beta_{2i})\boldsymbol{j}_0 + cos(\beta_{2i})\boldsymbol{k}_0 \tag{25}$$

The kinematic variables can be found as:

$$\beta_{2i} = cos^{-1}(n_{iz}) \tag{26}$$

$$\beta_{1i} = atan2(\sigma n_{iy}; \sigma n_{ix}), \; \sigma = sgn(sin(\beta_{2i})) \tag{27}$$

The expression for β_{1i} in equation (27) is not defined if $sin(\beta_{2i})=0$, i.e., at $\beta_{2i}=0,\pi$ so that $\boldsymbol{n}_i=\pm\boldsymbol{k}_0$. In this case β_{1i} can be any arbitrary value. The orientation of the mobile platform can also be written in terms of the kinematic variables used to define the motion of the wires. Hence, using *zyx* (roll-pitch-yaw) Euler angle sequence for describing the spherical motion of wires 1 and 2 at their attachment points to the mobile platform, the orientation of the mobile platform can be found. For wire 3, which is connected to link 5, the orientation of link 5 is used instead of the mobile platform. The orientation of the mobile platform can be written as:

$$\boldsymbol{R}_{0,m}=e^{\tilde{k}\beta_{1i}}\,e^{\tilde{j}\beta_{2i}}\,e^{\tilde{k}\beta_{3i}}\,e^{\tilde{j}\beta_{4i}}\,e^{\tilde{i}\beta_{5i}}=e^{\tilde{k}\gamma} \tag{28}$$

After calculating β_{1i} and β_{2i}, equation (28) can be rearranged such that the known terms are collected in the right-hand side and called as matrix $\boldsymbol{R}^*$ as $e^{\tilde{k}\beta_{3i}}\,e^{\tilde{j}\beta_{4i}}\,e^{\tilde{i}\beta_{5i}}=e^{-\tilde{j}\beta_{2i}}\,e^{-\tilde{i}\beta_{1i}}\,e^{\tilde{k}\gamma}=\boldsymbol{R}_i^*$. For example, the orientation of wire 3 can be obtained by using the orientation of the link 5 as:

$$\beta_{4i}=atan2\left(-r_{31i}^*;\sigma_1\sqrt{1-r_{31i}^{*\,2}}\right),\ \sigma_1=\pm1 \tag{29}$$

$$\beta_{3i}=atan2\left(\sigma r_{21i}^*;\sigma r_{11i}^*\right),\ \sigma=sgn(cos(\beta_{4i})) \tag{30}$$

$$\beta_{5i}=atan2\left(\sigma r_{32}^*;\sigma r_{33}^*\right) \tag{31}$$

where $r_{31i}^*=-sin(\beta_{4i})$, $r_{11i}^*=cos(\beta_{3i})cos(\beta_{4i})$, $r_{21i}^*=sin(\beta_{3i})cos(\beta_{4i})$, $r_{32i}^*=cos(\beta_{4i})sin(\beta_{5i})$, $r_{33i}^*=cos(\beta_{4i})cos(\beta_{5i})$, and r_{kji}^* denotes the elements of the rotation matrix $\boldsymbol{R}_i^*$ for wire *i*. It should be noted that the expressions for β_{3i} and β_{5i} are not defined if $cos(\beta_{4i})=0$ so that $\beta_{4i}=\pm\pi/2$. Inspecting the elements of the rotation matrix $\boldsymbol{R}_i$, in this case the summation $\beta_{3i}+\beta_{5i}$ can be found. Other Euler angle sequences such as *zyz* can be used as an alternative to the *zyx* sequential rotations when the singularity of roll-pitch-yaw occurs.

2.3. Workspace Analysis

The workspace of a manipulator can be investigated using either the forward or inverse position analysis. The forward position analysis can be used for obtaining the workspace of the manipulator by varying the joint variables within their limits. The maximum and the minimum values of the position can be stored to obtain the workspace. Alternatively, choosing points in the Cartesian space, the inverse position analysis could be performed to identify the points that lie in the workspace of manipulator. The workspace of the wire-actuated parallel manipulator is investigated based on the inverse position analysis formulated in Section 2.2. A computer program is written in Matlab to obtain the workspace using cylindrical coordinates by identifying the internal and external boundaries of the workspace in planes parallel to the horizontal plane (Y_0Z_0 plane) within a defined minimum and maximum elevation of the mobile platform (in the X_0 direction). The input to the program includes the lower and upper elevation for the mobile platform, and minimum and maximum values for the search radius and angle.

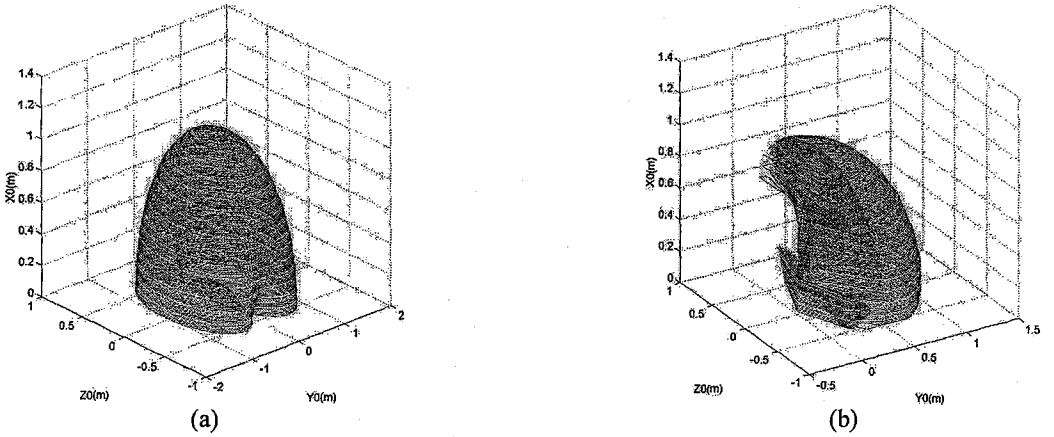

(a) (b)

Figure 4 Workspace of the wire-actuated parallel manipulator (a) simulated one (b) prototyped one.

To identify the internal and external boundaries, the calculated joint variables and wire lengths are compared with the allowable joint ranges of $0 \le \theta_i \le 2\pi$ for $i = 1,6,7$ and $-\pi/2 \le \theta_2 \le \pi/2$, and the maximum wire lengths, to verify that the point can be reached. In the internal search algorithm, for a search angle, the radius is incremented starting from zero and the value for the first reachable point for that angle is recorded in an array. In the external boundary search, the array of radii obtained as the internal boundary is used as the initial search radii. Then, for each value of the search angle, the radius is incremented until a point, which is outside the workspace, is identified. Then, the point before that, inside the workspace, is collected. The radii collected from this procedure are recorded in another array. The workspace of the manipulator, is illustrated in Figure 4(a), is obtained after recording the internal and external boundaries of the workspace in planes parallel to the Y_0Z_0 plane for the incremented coordinates in the X_0 direction. The simulation program allows the possible joint limitations because of the link/wire interference. To illustrate this, another simulation is performed with constraints of the prototyped manipulator, i.e., $-\pi/36 \le \theta_1 \le 7\pi/18$, $-7\pi/18 \le \theta_2 \le 7\pi/18$ and $-8\pi/9 \le \theta_6 \le 8\pi/9$. The result is shown in Figure 4(b).

2.4. Velocity Analysis

Rigid Branch

The Jacobian matrix of the rigid branch can be formulated using its position and orientation equations. The time derivative of equation (12), $D_0(d_1 k_0) + D_0(a_2 i_2) - 2D_0(d_6 k_3) = D_0(-d_1 k_0) + D_0(a_4 i_4)$, is simplified as:

2.4. Velocity Analysis

Rigid Branch

The Jacobian matrix of the rigid branch can be formulated using its position and orientation equations. The time derivative of equation (12), $D_0(d_1 k_0) + D_0(a_2 i_2) - 2D_0(d_6 k_3) = D_0(-d_1 k_0) + D_0(a_4 i_4)$, is simplified as:

$$w_{2/0} \times a_2 i_2 - 2 w_{3/0} \times d_6 k_3 = w_{4/0} \times a_4 i_4 \tag{32}$$

where $w_{2/0} = \dot{\theta}_1 k_0 + \dot{\theta}_2 k_1$, $w_{3/0} = \dot{\theta}_1 k_0 + \dot{\theta}_2 k_1 + \dot{\theta}_3 k_2$, and $w_{4/0} = \dot{\theta}_1 k_0 + \dot{\theta}_5 k_5$. Then using rotation matrices $R_{0,1} = e^{\tilde{k}\theta_1} e^{\tilde{i}\frac{\pi}{2}}$ and $R_{0,5} = e^{\tilde{k}\theta_1} e^{\tilde{i}\frac{\pi}{2}} e^{\tilde{k}\theta_5}$, and defining $J_{\theta_1} = a_2 \tilde{k} e^{\tilde{i}\frac{\pi}{2}} e^{\tilde{k}\theta_2} i - 2 d_6 \tilde{k} e^{-\tilde{j}\theta_{23}} k - a_4 \tilde{k} e^{\tilde{i}\frac{\pi}{2}} e^{\tilde{k}\theta_5} i$, $J_{\theta_2} = a_2 e^{\tilde{i}\frac{\pi}{2}} \tilde{k} e^{\tilde{k}\theta_2} i + 2 d_6 e^{\tilde{i}\frac{\pi}{2}} \tilde{j} e^{-\tilde{j}\theta_{23}} k$, $J_{\theta_3} = 2 d_6 e^{\tilde{i}\frac{\pi}{2}} \tilde{j} e^{-\tilde{j}\theta_{23}} k$ and $J_{\theta_5} = -a_4 e^{\tilde{i}\frac{\pi}{2}} \tilde{k} e^{\tilde{k}\theta_5} i$, a matrix equation can be found as:

$$J_{\theta_1} \dot{\theta}_1 + J_{\theta_2} \dot{\theta}_2 + J_{\theta_3} \dot{\theta}_3 + J_{\theta_5} \dot{\theta}_5 = 0 \tag{33}$$

Simplifying this equation using the equality of link lengths and the relations between the joint variables of the parallelogram mechanism, the relation between the joint velocities can be obtained as:

$$\begin{bmatrix} \dot{\theta}_3 \\ \dot{\theta}_5 \end{bmatrix} = \left(J_p^{-1} J_a \right) \begin{bmatrix} \dot{\theta}_1 \\ \dot{\theta}_2 \end{bmatrix} = \begin{bmatrix} 0 & -1 \\ 0 & 1 \end{bmatrix} \begin{bmatrix} \dot{\theta}_1 \\ \dot{\theta}_2 \end{bmatrix} \tag{34}$$

where J_p^{-1} and J_a are constructed from the two scalar independent equations of equation (33).

Taking into account that $\dot{\theta}_4 = \dot{\theta}_3 = -\dot{\theta}_2$, the passive joint velocities $(\dot{\theta}_3, \dot{\theta}_4, \dot{\theta}_5)$ of the parallelogram mechanism can be related to the active joint velocities $(\dot{\theta}_1, \dot{\theta}_2)$ by a Jacobian matrix J_a^p as:

$$\begin{bmatrix} \dot{\theta}_3 \\ \dot{\theta}_4 \\ \dot{\theta}_5 \end{bmatrix} = \begin{bmatrix} 0 & -1 \\ 0 & -1 \\ 0 & 1 \end{bmatrix} \begin{bmatrix} \dot{\theta}_1 \\ \dot{\theta}_2 \end{bmatrix} = J_a^p \begin{bmatrix} \dot{\theta}_1 \\ \dot{\theta}_2 \end{bmatrix} \tag{35}$$

The linear velocity of the mobile platform (origin of frame 7) in terms of the joint velocities of the constraining branch can be written as $v_{O_7} = D_0(d_1 k_0) + D_0(a_2 i_2) - D_0(d_6 k_3) + D_0(a_6 i_6)$ and simplified as:

$$v_{O_7} = w_{2/0} \times a_2 i_2 - w_{3/0} \times d_6 k_3 + w_{6/0} \times a_6 i_6 \tag{36}$$

where $w_{6/0} = \dot{\theta}_1 k_0 + \dot{\theta}_2 k_1 + \dot{\theta}_3 k_2 + \dot{\theta}_6 k_3$. The angular velocity of the mobile platform can be written as:

$$\boldsymbol{w} = \dot{\theta}_1 \boldsymbol{k}_0 + \dot{\theta}_2 \boldsymbol{k}_1 + \dot{\theta}_3 \boldsymbol{k}_2 + \dot{\theta}_6 \boldsymbol{k}_3 + \dot{\theta}_7 \boldsymbol{k}_6 \tag{37}$$

The velocity equation of the mobile platform can be resolved into the fixed frame as:

$$\begin{bmatrix} {}^0\boldsymbol{v}_{O_7} \\ {}^0\boldsymbol{w} \end{bmatrix} = \boldsymbol{J}_{rb} \begin{bmatrix} \dot{\theta}_1 \\ \dot{\theta}_2 \\ \dot{\theta}_6 \\ \dot{\theta}_7 \end{bmatrix}, \quad \boldsymbol{J}_{rb} = \begin{bmatrix} -a_2 c\theta_2 s\theta_1 - a_6 s\theta_{16} & -a_2 c\theta_1 s\theta_2 & -a_6 s\theta_{16} & 0 \\ a_2 c\theta_2 c\theta_1 + a_6 c\theta_{16} & -a_2 s\theta_1 s\theta_2 & a_6 c\theta_{16} & 0 \\ 0 & a_2 c\theta_2 & 0 & 0 \\ 1 & 0 & 1 & 1 \end{bmatrix} \tag{38}$$

The tip point Jacobian matrix relates the velocity $\begin{bmatrix} {}^0\boldsymbol{v}^T & {}^0\boldsymbol{w}^T \end{bmatrix}^T$ of the point of application of the external wrench on the mobile platform to the fixed frame, as:

$$\begin{bmatrix} {}^0\boldsymbol{v} \\ {}^0\boldsymbol{w} \end{bmatrix} = \begin{bmatrix} \boldsymbol{I} & \boldsymbol{R}_{0,7}\, {}^7\tilde{\boldsymbol{p}}_{O_7,P} \\ \boldsymbol{0} & \boldsymbol{I} \end{bmatrix} \begin{bmatrix} {}^0\boldsymbol{v}_{O_7} \\ {}^0\boldsymbol{w} \end{bmatrix} \tag{39}$$

where $\boldsymbol{p}_{O_7,P}$ is the displacement vector from the origin of the mobile platform coordinate frame to the point of application of the external wrench.

The independent joint velocities of the rigid branch can be calculated as:

$$\begin{bmatrix} \dot{\theta}_1 \\ \dot{\theta}_2 \\ \dot{\theta}_6 \\ \dot{\theta}_7 \end{bmatrix} = \boldsymbol{J}^{\#} \begin{bmatrix} {}^0\boldsymbol{v} \\ {}^0\boldsymbol{w} \end{bmatrix} \tag{40}$$

where $\boldsymbol{J}^{\#}$ is the 4×6 generalized inverse of the Jacobian matrix.

The velocity of the dependent joints of the parallelogram mechanism is obtained using equations (35) and (40) as:

$$\begin{bmatrix} \dot{\theta}_3 \\ \dot{\theta}_4 \\ \dot{\theta}_5 \end{bmatrix} = \boldsymbol{J}_a^p \begin{bmatrix} \dot{\theta}_1 \\ \dot{\theta}_2 \end{bmatrix} = \boldsymbol{J}_a^p \begin{bmatrix} \left(\boldsymbol{J}^{\#}\right)_{1r} \\ \left(\boldsymbol{J}^{\#}\right)_{2r} \end{bmatrix} \begin{bmatrix} {}^0\boldsymbol{v} \\ {}^0\boldsymbol{w} \end{bmatrix} = \boldsymbol{J}_a^m \begin{bmatrix} {}^0\boldsymbol{v} \\ {}^0\boldsymbol{w} \end{bmatrix}, \; r = 1,\ldots,6 \tag{41}$$

where the 3×6 Jacobian matrix $\boldsymbol{J}_a^m$ relates the dependent joint rates to the velocity of the mobile platform. The first two rows of the generalized inverse Jacobian matrix of the rigid branch, $\left(\boldsymbol{J}^{\#}\right)_{1r}$, $\left(\boldsymbol{J}^{\#}\right)_{2r}$, are used to obtain $\boldsymbol{J}_a^m$. Thus, all the joint velocities in the rigid branch are related to the task space coordinates.

Wire Mechanism

The first order kinematics of the wires can be performed by utilizing the loop closure equations. Differentiating the loop closure equations for wires 1 and 2:

$$\dot{\boldsymbol{l}}_i + \boldsymbol{w}_{2wi} \times \boldsymbol{l}_i = \boldsymbol{v} + \boldsymbol{w} \times \boldsymbol{r}_{O_7 B_i} \tag{42}$$

where $\dot{l}_i$ is the time rate of change in the length of wire i, $\boldsymbol{w}_{2wi} = \dot{\beta}_{1i} \boldsymbol{k}_0 + \dot{\beta}_{2i} \boldsymbol{j}_1$, $\boldsymbol{w} = \dot{\beta}_{1i} \boldsymbol{k}_0 + \dot{\beta}_{2i} \boldsymbol{j}_1 + \dot{\beta}_{3i} \boldsymbol{k}_2 + \dot{\beta}_{4i} \boldsymbol{j}_3 + \dot{\beta}_{5i} \boldsymbol{i}_4$ is the angular velocity and $\boldsymbol{v}$ is the linear velocity of the mobile platform. Equations (42) can be arranged to obtain:

$$\dot{\boldsymbol{q}}_{wi} = \left(\boldsymbol{J}_{wi}\right)^{-1} \boldsymbol{J}_m \begin{bmatrix} {}^0\boldsymbol{v}_{O_7} \\ {}^0\boldsymbol{w} \end{bmatrix} = \boldsymbol{J}_m^{wi} \begin{bmatrix} {}^0\boldsymbol{v}_{O_7} \\ {}^0\boldsymbol{w} \end{bmatrix} \tag{43}$$

where $\dot{\boldsymbol{q}}_{wi} = \begin{bmatrix} \dot{\beta}_{1i} & \dot{\beta}_{2i} & \dot{l}_i & \dot{\beta}_{3i} & \dot{\beta}_{4i} & \dot{\beta}_{5i} \end{bmatrix}^T$ is a vector composed of the time rate of change of the wire parameters,

$\boldsymbol{J}_{wi} = \begin{bmatrix} \tilde{\boldsymbol{k}}_{0i}\, {}^0\boldsymbol{l}_i & \boldsymbol{R}_{0,1i}\, \tilde{\boldsymbol{j}}\, {}^0\boldsymbol{l}_i & {}^0\boldsymbol{n}_i & \boldsymbol{0} & \boldsymbol{0} & \boldsymbol{0} \\ \boldsymbol{k}_{0i} & \boldsymbol{R}_{0,1i}\, \boldsymbol{j} & \boldsymbol{0} & \boldsymbol{R}_{0,2i}\, \boldsymbol{k} & \boldsymbol{R}_{0,3i}\, \boldsymbol{j} & \boldsymbol{R}_{0,4i}\, \boldsymbol{i} \end{bmatrix}$ and $\boldsymbol{J}_m = \begin{bmatrix} \boldsymbol{I} & -\boldsymbol{R}_{0,m}\, \tilde{\boldsymbol{p}}_{O_7 B_i} \\ \boldsymbol{0} & \boldsymbol{I} \end{bmatrix}$ are respectively the Jacobian matrices related to the kinematic variables of wire i and to the velocity of the mobile platform. The Jacobian matrix relating the point of application of the external wrench to the wire velocity is:

$$\begin{bmatrix} {}^0\boldsymbol{v} \\ {}^0\boldsymbol{w} \end{bmatrix} = \begin{bmatrix} \boldsymbol{I} & -\boldsymbol{R}_{0,m}\,\tilde{\boldsymbol{p}}_{O_7P} \\ \boldsymbol{0} & \boldsymbol{I} \end{bmatrix} \left(\boldsymbol{J}_m^{wi}\right)^{-1} \dot{\boldsymbol{q}}_{wi} = \boldsymbol{J}_{wi}^{p}\,\dot{\boldsymbol{q}}_{wi} \tag{44}$$

The velocity equation for wire 3 can also be obtained by differentiating its loop closure equation as:

$$\dot{\boldsymbol{l}}_3 + \boldsymbol{w}_{2w3} \times \boldsymbol{l}_3 = \boldsymbol{v}_{O_7} - \boldsymbol{w}_{6/0} \times \left(\boldsymbol{a}_6 + \boldsymbol{a}_{6p}\right)\boldsymbol{i}_6 \tag{45}$$

where $a_{6p} = \|\boldsymbol{CB}_3\|$ is the distance from the attachment point of wire 3 to point C on link 5 with its frame labelled as frame 6, and $\boldsymbol{w}_{6/0} = \dot{\beta}_{13}\,\boldsymbol{k}_0 + \dot{\beta}_{23}\,\boldsymbol{j}_1 + \dot{\beta}_{33}\,\boldsymbol{k}_2 + \dot{\beta}_{43}\,\boldsymbol{j}_3 + \dot{\beta}_{53}\,\boldsymbol{i}_4 = \left(\dot{\theta}_1 + \dot{\theta}_6\right)\boldsymbol{k}_0$ is the angular velocity of link 5 with respect to the fixed coordinate frame. To relate the wire velocity to the mobile platform velocity, equation (44) is used with different expression for $\boldsymbol{J}_m$, which is obtained by eliminating the intermediate joint rates $\dot{\theta}_6$ and $\dot{\theta}_7$ as $\boldsymbol{J}_m = \begin{bmatrix} \boldsymbol{I} & \boldsymbol{0} \\ \boldsymbol{0} & \boldsymbol{0} \end{bmatrix} + \begin{bmatrix} -\left(\boldsymbol{a}_6 + \boldsymbol{a}_{6p}\right)\left(\tilde{\boldsymbol{k}}_0\,\boldsymbol{R}_{0,6}\,\boldsymbol{i}_6\right)\left(\left(\boldsymbol{J}^{\#}\right)_{1r} + \left(\boldsymbol{J}^{\#}\right)_{3r}\right) \\ \boldsymbol{k}_0\left(\left(\boldsymbol{J}^{\#}\right)_{1r} + \left(\boldsymbol{J}^{\#}\right)_{3r}\right) \end{bmatrix}$. The tip point Jacobian matrix can also be found for the third wire using equation (44).

Any set of velocities, e.g., active, passive or task space velocities of the manipulator can be related to another by using the Jacobian matrices formulated in this section. For example, the velocity of active joints and time rate of change of wire lengths $\dot{\boldsymbol{q}}_a = \begin{bmatrix} \dot{\theta}_1 & \dot{\theta}_2 & \dot{l}_1 & \dot{l}_2 & \dot{l}_3 \end{bmatrix}^T$ can be related to the velocity of mobile platform by extracting the associated rows of the Jacobian matrices from $\boldsymbol{J}^{\#}$, $\boldsymbol{J}_{wi}^{p}$ $i = 1 \ldots 3$, via a 5×6 Jacobian matrix $\boldsymbol{J}_m^a$ as:

$$\dot{\boldsymbol{q}}_a = \boldsymbol{J}_m^a \begin{bmatrix} {}^0\boldsymbol{v} \\ {}^0\boldsymbol{w} \end{bmatrix} = \begin{bmatrix} \left(\boldsymbol{J}^{\#}\right)_{1r} \\ \left(\boldsymbol{J}^{\#}\right)_{2r} \\ \left(\boldsymbol{J}_{w1}^{p}\right)_{3r} \\ \left(\boldsymbol{J}_{w2}^{p}\right)_{3r} \\ \left(\boldsymbol{J}_{w3}^{p}\right)_{3r} \end{bmatrix} \begin{bmatrix} {}^0\boldsymbol{v} \\ {}^0\boldsymbol{w} \end{bmatrix} \tag{46}$$

2.5. Acceleration Analysis

Rigid Branch

The acceleration of the passive joints in the parallelogram mechanism can be related to the acceleration of the active joints. Using the angular accelerations of links; $\boldsymbol{\alpha}_{2/0} = D_0\left(\boldsymbol{w}_{2/0}\right) = \ddot{\theta}_1\,\boldsymbol{k}_0 + \ddot{\theta}_2\,\boldsymbol{k}_1 + \boldsymbol{w}_{1/0} \times \left(\dot{\theta}_2\,\boldsymbol{k}_1\right)$, $\boldsymbol{\alpha}_{3/0} = D_0\left(\boldsymbol{w}_{3/0}\right) = \ddot{\theta}_1\,\boldsymbol{k}_0 + \ddot{\theta}_2\,\boldsymbol{k}_1 + \boldsymbol{w}_{1/0} \times \left(\dot{\theta}_2\,\boldsymbol{k}_1\right) + \ddot{\theta}_3\,\boldsymbol{k}_2 + \boldsymbol{w}_{2/0} \times \left(\dot{\theta}_3\,\boldsymbol{k}_2\right)$, $\boldsymbol{\alpha}_{4/0} = D_0\left(\boldsymbol{w}_{4/0}\right) = \ddot{\theta}_1\,\boldsymbol{k}_0 + \ddot{\theta}_5\,\boldsymbol{k}_5 + \boldsymbol{w}_{5/0} \times \left(\dot{\theta}_5\,\boldsymbol{k}_5\right)$; the second derivative of equation (12), $D_0^2\left(d_1\,\boldsymbol{k}_0\right) + D_0^2\left(a_2\,\boldsymbol{i}_2\right) + D_0^2\left(-2\,d_3\,\boldsymbol{k}_3\right) = D_0^2\left(-d_1\,\boldsymbol{k}_0\right) + D_0^2\left(a_4\,\boldsymbol{i}_4\right)$, is simplified as:

$$\begin{aligned} &\boldsymbol{\alpha}_{2/0} \times \left(a_2\,\boldsymbol{i}_2\right) + \boldsymbol{w}_{2/0} \times \left(\boldsymbol{w}_{2/0} \times \left(a_2\,\boldsymbol{i}_2\right)\right) + \boldsymbol{\alpha}_{3/0} \times \left(-2\,d_6\,\boldsymbol{k}_3\right) + \boldsymbol{w}_{3/0} \times \left(\boldsymbol{w}_{3/0} \times \left(-2\,d_6\,\boldsymbol{k}_3\right)\right) = \\ &\quad \boldsymbol{\alpha}_{4/0} \times \left(a_4\,\boldsymbol{i}_4\right) + \boldsymbol{w}_{4/0} \times \left(\boldsymbol{w}_{4/0} \times \left(a_4\,\boldsymbol{i}_4\right)\right) \end{aligned} \tag{47}$$

The relation between the active and passive joint accelerations of the parallelogram mechanism can be obtained as:

$$\begin{bmatrix} \ddot{\theta}_3 \\ \ddot{\theta}_4 \\ \ddot{\theta}_5 \end{bmatrix} = \begin{bmatrix} 0 & -1 \\ 0 & -1 \\ 0 & 1 \end{bmatrix} \begin{bmatrix} \ddot{\theta}_1 \\ \ddot{\theta}_2 \end{bmatrix} = \boldsymbol{J}_a^p \begin{bmatrix} \ddot{\theta}_1 \\ \ddot{\theta}_2 \end{bmatrix} \tag{48}$$

The mass centre accelerations of the moving links in the parallelogram mechanism can be calculated as:

$$\boldsymbol{a}_{G_2} = D_0\left(\boldsymbol{v}_{G_2}\right) = \boldsymbol{\alpha}_{2/0} \times \left(r_{G_2}\,\boldsymbol{i}_2\right) + \boldsymbol{w}_{2/0} \times \left(\boldsymbol{w}_{2/0} \times \left(r_{G_2}\,\boldsymbol{i}_2\right)\right) \tag{49}$$

$$\boldsymbol{a}_{G_3} = D_0\left(\boldsymbol{v}_{G_3}\right) = \boldsymbol{\alpha}_{2/0} \times \left(a_2\boldsymbol{i}_2\right) + \boldsymbol{w}_{2/0} \times \left(\boldsymbol{w}_{2/0} \times \left(a_2\boldsymbol{i}_2\right)\right) + \boldsymbol{\alpha}_{3/0} \times \left(-r_{G_3}\boldsymbol{k}_3\right) + \boldsymbol{w}_{3/0} \times \left(\boldsymbol{w}_{3/0} \times \left(-r_{G_3}\boldsymbol{k}_3\right)\right) \tag{50}$$

$$\boldsymbol{a}_{G_4} = D_0\left(\boldsymbol{v}_{G_4}\right) = \boldsymbol{\alpha}_{4/0} \times \left(r_{G_4}\,\boldsymbol{i}_4\right) + \boldsymbol{w}_{4/0} \times \left(\boldsymbol{w}_{4/0} \times \left(r_{G_4}\,\boldsymbol{i}_2\right)\right) \tag{51}$$

where r_{G_i} represents the distance of the mass centre of link i from the origin of its coordinate system.

The linear and angular accelerations of the mobile platform can be written in terms of the acceleration of the joint variables by differentiating equations (36) and (37) as follows:

$$\boldsymbol{a}_{O_7} = \boldsymbol{\alpha}_{2/0} \times (a_2 \boldsymbol{i}_2) + \boldsymbol{w}_{2/0} \times (\boldsymbol{w}_{2/0} \times (a_2 \boldsymbol{i}_2)) - \boldsymbol{\alpha}_{3/0} \times (d_6 \boldsymbol{k}_3) - \boldsymbol{w}_{3/0} \times (\boldsymbol{w}_{3/0} \times (d_6 \boldsymbol{k}_3)) + \boldsymbol{\alpha}_{6/0} \times (a_6 \boldsymbol{i}_6) + \boldsymbol{w}_{6/0} \times (\boldsymbol{w}_{6/0} \times (a_6 \boldsymbol{i}_6)) \tag{52}$$

$$\boldsymbol{\alpha}_{7/0} = \ddot{\theta}_1 \boldsymbol{k}_0 + \ddot{\theta}_2 \boldsymbol{k}_1 + \boldsymbol{w}_{1/0} \times \dot{\theta}_2 \boldsymbol{k}_1 + \ddot{\theta}_3 \boldsymbol{k}_2 + \boldsymbol{w}_{2/0} \times \dot{\theta}_3 \boldsymbol{k}_2 + \ddot{\theta}_6 \boldsymbol{k}_3 + \boldsymbol{w}_{3/0} \times \dot{\theta}_6 \boldsymbol{k}_3 + \ddot{\theta}_7 \boldsymbol{k}_6 + \boldsymbol{w}_{6/0} \times \dot{\theta}_7 \boldsymbol{k}_6 \tag{53}$$

where $\boldsymbol{\alpha}_{6/0} = \ddot{\theta}_1 \boldsymbol{k}_0 + \ddot{\theta}_2 \boldsymbol{k}_1 + \boldsymbol{w}_{1/0} \times \dot{\theta}_2 \boldsymbol{k}_1 + \ddot{\theta}_3 \boldsymbol{k}_2 + \boldsymbol{w}_{2/0} \times \dot{\theta}_3 \boldsymbol{k}_2 + \ddot{\theta}_6 \boldsymbol{k}_3 + \boldsymbol{w}_{3/0} \times \dot{\theta}_6 \boldsymbol{k}_3$. Equations (52) and (53) can be resolved into the fixed frame and simplified by using the results of the position and velocity analyses to obtain a relationship between the angular acceleration of joints and the acceleration of the mobile platform as:

$$\begin{bmatrix} \boldsymbol{a}_m \\ \boldsymbol{\alpha}_m \end{bmatrix} = \boldsymbol{J}_{tp} \ddot{\boldsymbol{q}}_{rb} + \dot{\boldsymbol{q}}_{rb}^T \boldsymbol{G} \dot{\boldsymbol{q}}_{rb} \tag{54}$$

The expression for the three dimensional matrix $\boldsymbol{G}$ is given in [19].The joint acceleration can be written in terms of the mobile platform acceleration as:

$$\ddot{\boldsymbol{q}} = \boldsymbol{J}_{tp}^{\#} \begin{bmatrix} \boldsymbol{a}_m \\ \boldsymbol{\alpha}_m \end{bmatrix} + \begin{bmatrix} \boldsymbol{a}_m^T & \boldsymbol{\alpha}_m^T \end{bmatrix} \boldsymbol{J}_{tp}^{\#} \circ \left(\boldsymbol{J}_{tp}^{\#T} \boldsymbol{G} \boldsymbol{J}_{tp}^{\#} \right) \begin{bmatrix} \boldsymbol{a}_m \\ \boldsymbol{\alpha}_m \end{bmatrix} \tag{55}$$

where the generalized tensor product $\boldsymbol{A} \circ \boldsymbol{B} = a_{ij} b_{jkl}$ is used in equation (55) (the quadratic term) so that the dimension of $\boldsymbol{J}_{tp}^{\#} \circ \left(\boldsymbol{J}_{tp}^{\#T} \boldsymbol{G} \boldsymbol{J}_{tp}^{\#} \right)$ is $4 \times 6 \times 6$. Mass centre acceleration of the mobile platform can be obtained by using the results of the acceleration analysis of the origin of the mobile platform coordinate frame. Thus,

$$\boldsymbol{a}_{G_7} = \boldsymbol{a}_{7/0} + \boldsymbol{\alpha}_{7/0} \times \boldsymbol{r}_{O_7 G_7} + \boldsymbol{w}_{7/0} \times \left(\boldsymbol{w}_{7/0} \times \boldsymbol{r}_{O_7 G_7} \right) \tag{56}$$

Wire Mechanism

The acceleration analysis of the wires can be performed by differentiating loop closure equations. Differentiating equation (42) and simplifying, the acceleration of the mobile platform can be written in terms of the velocity and acceleration of wires 1 and 2 (attached to the mobile platform) as:

$$\boldsymbol{J}_{qwi} \ddot{\boldsymbol{q}}_{wi} = \boldsymbol{J}_m^{wi} \begin{bmatrix} {}^0\boldsymbol{a}_{O_7} \\ {}^0\boldsymbol{\alpha} \end{bmatrix} + \dot{\boldsymbol{q}}_{wi}{}^T \boldsymbol{G}_{wi} \dot{\boldsymbol{q}}_{wi} \ , \ i = 1,2 \tag{57}$$

The three-tensor in the quadratic term of equation (57) is derived as follows. The first three matrices of the three dimensional array $\boldsymbol{G}_{wi}$ are calculated from the linear accelerations by resolving the Coriolis and centripetal acceleration terms into the fixed frame:

$$Q_{awi} = \sum_{r=1}^{6} \sum_{j=1}^{6} \dot{q}_{wir} \left(\tilde{\boldsymbol{e}}_i^r \tilde{\boldsymbol{r}}_{O_7 B_i} \boldsymbol{e}_i^j \right) \dot{q}_{jwi} - 2 \sum_{r=1}^{2} \dot{q}_{wir} \left(\tilde{\boldsymbol{e}}_i^r \boldsymbol{e}_i^3 \right) \dot{q}_{wi3} - \sum_{r=1}^{2} \sum_{j=1}^{2} \dot{q}_{wir} \left(\tilde{\boldsymbol{e}}_i^r \tilde{\boldsymbol{l}}_i \boldsymbol{e}_i^j \right) \dot{q}_{wij} \tag{58}$$

where the indicial notation is preferred to represent the quadratic form. The tensors in equation (58), $\boldsymbol{e}_i^j$, $j = 1,\ldots,6$, are the upper three entries of the j^{th} column of $\boldsymbol{J}_{qwi}$. Denoting the tensors inside the quadratics as $\boldsymbol{a}_i^{rj} = \tilde{\boldsymbol{e}}_i^r \tilde{\boldsymbol{r}}_{O_7 B_i} \boldsymbol{e}_i^j$, $\boldsymbol{b}_i^{r3} = 2 \tilde{\boldsymbol{e}}_i^r \boldsymbol{e}_i^3$, $c_i^{kn} = \tilde{\boldsymbol{e}}_i^k \tilde{\boldsymbol{l}}_i \boldsymbol{e}_i^n$; the three matrices of $\boldsymbol{G}_{wi}$ can be written in tensorial form as:

$$g_{swi}^{rj} = a_s^{rj} - b_s^{rj} - c_s^{rj} \ , \ s = 1,\ldots,3 \tag{59}$$

The nonzero entities of g_{swi}^{rj} related to indices r, j are of dimension 2; they are increased to 6 (dimension of the vector of kinematic variables of wires) by adding zeros. Thus, three of the 6×6 matrices in the s^{th} index of $\boldsymbol{G}_{wi}$ are obtained. The last three matrices of $\boldsymbol{G}_{wi}$ are calculated from the angular acceleration. Detailed expressions of $\boldsymbol{G}_{wi}$ are included in [19].

The acceleration of wire 3 is related to the mobile platform by taking the time derivative of equation (45) using $\boldsymbol{J}_{\theta_6}^w = \begin{bmatrix} (a_6 + a_{6p}) \boldsymbol{R}_{0,6} \boldsymbol{j} \\ \boldsymbol{R}_{0,6} \boldsymbol{k} \end{bmatrix}$:

$$\boldsymbol{J}_{qw_3} \ddot{\boldsymbol{q}}_{w_3} = \boldsymbol{J}_m^w \begin{bmatrix} \boldsymbol{a}_m \\ \boldsymbol{\alpha}_m \end{bmatrix} + \dot{\boldsymbol{q}}_{w_3}{}^T \boldsymbol{G}_{w_3} \dot{\boldsymbol{q}}_{w_3} + \boldsymbol{J}_{\theta_6}^w \ddot{\theta}_6 + \dot{\boldsymbol{q}}_{w_3}{}^T \boldsymbol{G}_{w_3 2} \dot{\theta}_6 \tag{60}$$

The first three matrices of $6\times1\times1$ $G_{w_3 2}$ can be found as $G_{w_3 2} = (a_6 + a_{6p})\sum_{k=1}^{3} \tilde{e}_k R_{0,6}\, j$ while the last three terms can be found as $G_{w_3 2} = \sum_{k=1}^{3} \tilde{e}_k\, k_6$. The vectors e_k are respectively the upper parts and the lower parts of the k^{th} column of $J_m^{w_3}$ for the first and the last three matrices of $G_{w_3 2}$. Thus, any set of coordinates can be written in terms of another.

3. DISCUSSION AND CONCLUSIONS

In this article, the kinematic analysis of a wire-actuated parallel (closed-loop) manipulator was discussed. The mobility of manipulator was investigated. A group theoric approach to the rigid body motion was considered. Lie groups and algebras associated with the Lie groups, exponential maps and its application to kinematics were introduced briefly. In general, kinematic analysis of closed-loop manipulators requires establishing the relations among the passive and active joint variables and task space coordinates. A framework for the kinematic (displacement, velocity and acceleration) analysis of closed-loop manipulators based on the matrix exponentials and transfer of coordinates was introduced and applied on a 4 DOF wire-actuated parallel manipulator. The matrix exponentials provide a compact representation of the equations for expressing kinematic equations, and the rich algebraic properties of the matrix exponentials give a more suitable basis for manipulation and simplification of the kinematic equations. This methodology was used effectively to formulate the first and second order kinematics (velocity and acceleration) of the manipulator, and map the corresponding kinematic variables between the generalized coordinates, the taskspace coordinates and the passive joint coordinates of the manipulator. These formulations have been used in the force and stiffness analyses of the wire-actuated manipulator in [11, 12].

REFERENCES

[1] Gough, V.E., Contributions to Discussion of Papers on Research in Automobile Stability, Control and Tyre Performance, Proc. Auto Div. Inst. Mech. Eng, 1956-57.

[2] Stewart D., A Platform with Six Degrees of Freedom, Proc. Inst. Mechanical Engineers, 180(15):371-378, 1965.

[3] Merlet, J.-P., Parallel Robots, Kluwer Academic Publishers, 2000.

[4] Denavit, J., and Hartenberg, R.S., A Kinematic Notation for Lower-Pair Mechanisms Based on Matrices, Journal of Applied Mechanics, 215-221, June 1956.

[5] Angeles, J., Rational Kinematics, Springer-Verlag, 1988.

[6] Hunt, K.H., Kinematic Geometry of Mechanisms, Oxford University Press, 1991

[7] Sattinger, D.H., and Weaver, O. L., Lie Groups and Algebras with Applications to Physics, Geometry, and Mechanics, Springer-Verlag, 1986.

[8] Brockett, R.W., Robotic Manipulators and the Product of Exponentials Formula, Mathematical Theory of Networks and Systems, Springer-Verlag, 58:120-129, 1984.

[9] Murray, R.M., Li, Z., and Sastry, S.S., A Mathematical Introduction to Robotic Manipulation, CRC Press, 1994.

[10] Lipkin H., Duffy, J., Sir Robert Stawell Ball and methodologies of modern screw theory, Proc. Instn. of Mechanical Engineers, Journal of Mechanical Engineering Science, 216(C):1-11, 2002.

[11] Sahin, S., and Notash, L., Static Force Analysis of Mechanisms with Four-bar Linkages Based on Flexibility Conditions, special edition of *CSME Transactions*, 29(4):605-616, 2005.

[12] Sahin, S., and Notash, L., Stiffness Analysis of a Wire-Actuated Parallel Manipulator, *Proc. CSME Forum*, 11 pages, 2006.

[13] Mroz, G., and Notash, L., Design and Prototype of Parallel, Wire-Actuated Robots with a Constraining Linkage, J. Robotic Systems, 21(12):677-687, 2004.

[14] Bagci, C., Degrees of Freedom of Motion in Mechanisms, Transactions of the ASME, 140:148, 1971.

[15] Phillips, J., Freedom in Machinery, Introducing Screw Theory, Vol. 1, Cambridge University Press, 1984.

[16] Waldron, K.J., and Kinzel, G.L., Kinematics, Dynamics, and Design of Machinery, John Wiley, 2004.

[17] Angeles, J., The Degree of Freedom of Parallel Robots: A Group-Theoretic Approach, *Proc. IEEE Int. Conf. Robo. and Auto.*, pp. 1017-1023, 2005.

[18] Paul, R.P., Robot Manipulators: Mathematics, Programming, and Control; the Computer Control of Robot Manipulators, M.I.T. Press, 1981.

[19] Sahin, S., Kinematics, Force and Stiffness Analysis of Parallel Manipulators, Ph.D. Dissertation, Department of Mechanical and Materials Engineering, Queen's University, Kingston, Canada, 2006.